Preparation and Electrorheological Characteristics of Poly(*p*-phenylene)-Based Suspensions

In S. Sim, Ji W. Kim, and Hyoung J. Choi*

Department of Polymer Science and Engineering, Inha University, Inchon, 402-751, Korea

Chul A. Kim and Myung S. Jhon

Department of Chemical Engineering, Carnegie Mellon University, Pittsburgh, Pennsylvania 15213

Received August 22, 2000. Revised Manuscript Received December 29, 2000

Poly(*p*-phenylene) (PPP) particles were synthesized from a bulk polymerization of benzene and then doped with $FeCl_3$ in aqueous solution to control their electrical conductivity for their electrorheological (ER) application. Various concentrations of the aqueous $FeCl_3$ were implemented to investigate the effect of doping degree on ER performance, and the yield stress of an ER fluid, which is a typical characteristic of a Bingham fluid, was found to be related to both the applied electric field strength and the doping degree. A universal scaling function was introduced to collapse all of the data. From dynamic experiments, it was also found that the semiconducting PPP-based ER fluids exhibit characteristics of a viscoelastic solid, which increases with electric field strength and doping degree.

Introduction

The "electrorheological (ER) effect" refers to the abrupt, reversible change of viscosity in certain suspensions of 2−100 μm diameter particles in an insulating oil by imposition of an electric field. ER fluids are thereby considered one of the most promising "smart" materials.[1−4] The ER phenomenon is also related to the drastic change of other rheological properties (for example, yield stress and viscoelasticity) under applied electric fields. Since their first discovery, ER substances have been the objects of very intensive theoretical[5−8] and experimental research[9−12] due to various potential applications, such as electrically controlled shock absorbers and electromechanical clutches.[13,14]

The change of viscosity results from reorientation of dispersed particles whose initially random distribution transforms into a fibrillated or layered structure, giving rise to higher viscosity. This fibrillated particle structure is known to be caused by the dielectric constant mismatch of the particles and the insulating oil due to an electrostatic interaction between particles.[15] As a shear force is applied to the chain structures made of polarized particles, the structures will be deformed, inclined, and broken down when flow occurs. Furthermore, ER fluids under an externally applied electric field exhibit Bingham fluid behavior[16] (e.g., yield stress). The Bingham fluid equation has been used as the suitable rheological model for the steady shear behavior of many ER fluids as described below:[16]

$$\tau = \tau_y + \eta\dot{\gamma} \qquad \tau \geq \tau_y$$
$$\dot{\gamma} = 0 \qquad \tau < \tau_y \tag{1}$$

Here, τ_y is the yield stress, which is a function of an electric field, τ is the shear stress, $\dot{\gamma}$ is the shear rate, and η shear viscosity. The $\dot{\gamma} = 0$ in eq 1 can be noted that the extrapolation of $\dot{\gamma}$ to zero gives the dynamic yield stress τ_y^d under a controlled shear rate test. Considering ER phenomena on the microscale, a strain applied perpendicular to the electric field distorts and rebuilds fibers between electrodes, and the dissipating energy from deformation results in the increase of viscosity.

Most ER particles, especially in hydrous systems, are known to require the addition of small quantities of water or other polar additives such as surfactant to produce the ER behavior. Various wet-base ER materials, including corn starch,[17] silica gel,[18,19] mesoporous

* Corresponding author. Telephone (82)-32-860-7486; FAX (82)-32-865-5178; E-mail hjchoi@inha.ac.kr.

(1) Choi, H. J.; Kim, T. W.; Cho, M. S.; Kim, S. G.; Jhon, M. S. *Eur. Polym. J.* **1997**, *33*, 699.
(2) Halsey, T. C.; Martin, J. E.; Adolf, D. *Phys. Rev. Lett.* **1992**, *68*, 1519.
(3) Rankin, P. J.; Ginder, J. M.; Klingenberg, D. J. *Curr. Opin. Colloid Interface Sci.* **1998**, *3*, 373.
(4) Phule, P. P.; Ginder, J. M. *MRS Bull.* **1998**, *23*, 19.
(5) Conrad, H.; Wu, C. W.; Tang, X. *Int. J. Mod. Phys. B* **1999**, *13*, 1729.
(6) See, H. *J. Phys. D: Appl. Phys.* **2000**, *33*, 1625.
(7) Tao, R.; Jiang, Q. *Phys. Rev. Lett.* **1994**, *73*, 205.
(8) Hao, T.; Kawai, A.; Ikazaki, F. *Int. J. Mod. Phys. B* **1999**, *13*, 1758.
(9) Boissy, C.; Wu, C. W.; Fahmy, Y.; Conrad, H. *Int. J. Mod. Phys. B* **1999**, *13*, 1775.
(10) Chen, T.; Zitter, R. N.; Tao, R. *Phys. Rev. Lett.* **1992**, *68*, 2555.
(11) Wu, C. W.; Conrad, H. *J. Phys. D: Appl. Phys.* **1998**, *31*, 3403.
(12) Chu, S. H.; Lee, S. J.; Ahn, K. H. *J. Rheol.* **2000**, *44*, 105.
(13) Choi, S. B. *Int. J. Mod. Phys. B* **1999**, *13*, 2160.
(14) Brooks, D. A. *Int. J. Mod. Phys. B* **1999**, *13*, 2127.
(15) Halsey, T. C. *Science* **1992**, *258*, 761.
(16) Parthasarathy, M.; Klingenberg, D. J. *Mater. Sci. Eng.* **1996**, *R17*, 57.
(17) Kobayashi, K.; Ogura, J.; Kodama, R.; Sakai, T.; Sato, M. *Int. J. Mod. Phys. B* **1999**, *13*, 1940.

10.1021/cm000677l CCC: $20.00
Published on Web 03/14/2001

molecular sieve,[20] and cellulose,[21] have been investigated. In wet-base systems with hydrophilic particles, the particle chain structure develops by the migration of ions in the absorbed water. However, hydrous ER fluids possess their own various disadvantages in practical engineering applications caused by the presence of water. Thereby, various anhydrous ER fluids, including semiconducting polymer particles, have been developed to overcome these disadvantages. These new ER materials, which possess advantages of a wide working temperature range, reduced device abrasion, and a relatively low current density, have intrinsic charge carriers in either the bulk particles or their surfaces that can move locally under an applied electric field. Examples include dehydrated zeolite,[22−24] annealed diphenyldiacetylene,[25] and several semiconducting polymers, such as polyaniline,[26−30] copolyaniline,[31−33] poly(acene quinone) radicals,[34,35] polyphenylenediamine,[36] and polymer−clay nanocomposites.[37−39]

Poly(*p*-phenylene) (PPP), which has been extensively studied as a conducting material, has recently been found to show ER characteristics. Plocharski et al.[40] claimed that a detailed atomic mechanism of the ER effect should take into account ionic polarizability and ion movement in the suspended particle material using PPP doped with $FeCl_3$ from a nitromethane solution. On the other hand, Chin et al.[41] further studied the effect of surfactants on the yield stress behavior of PPP-based ER suspensions. Recently, Choi et al.[42] investigated an ER system with PPP particles doped with $FeCl_3$ in aqueous solution.

Table 1. Compositions of 10 wt % PPP Suspensions in Silicone Oil and Conductivities of the PPP Particles

code	doping degree	conductivity, S cm^{-1}
PPP(0.0)	undoped	1.12×10^{-13}
PPP(2.5)	2.5 wt % $FeCl_3$ in aqueous solution	1.44×10^{-12}
PPP(5.0)	5.0 wt % $FeCl_3$ in aqueous solution	4.40×10^{-10}
PPP(7.5)	7.5 wt % $FeCl_3$ in aqueous solution	1.12×10^{-9}

In this study, we synthesized PPP and then investigated the ER properties of its suspensions because of its high stability and relatively ease of doping at low concentrations. The yield stress of the ER fluid was studied as a function of electric field strength and doping degree. Furthermore, from the dynamic experiments, viscoelastic characterization of the ER fluid was also examined.

Experimental Section

Materials Synthesis and Structure Characterization. Semiconducting PPP particles were synthesized following the method of Kovacic and Oziomek.[43] Under a nitrogen atmosphere and in the presence of aluminum chloride, water, and cupric chloride, which forms a Lewis acid, benzene was converted to PPP. The polymerization temperature was kept at 45 °C. The stirring speed was maintained to be approximately 400−500 rpm for 2 h. After polymerization, the mixture was washed using water and ethyl alcohol to remove $CuCl_2$ and aqueous acid. The PPP was then dried and milled. To control the conductivity of the PPP particles, $FeCl_3$ solution was added as a dopant. Particles were doped with one of three different $FeCl_3$ concentrations in aqueous solution (2.5, 5.0, and 7.5 wt %) for 48 h. Unless specified, all measurements were performed at 25 ± 0.1 °C. After doping, the PPP particles were filtered and then dried vacuum for 2 days to remove any trace of water.

To determine the chemical structure of the synthesized PPP, FT-IR spectroscopy (Bruker IFS 48, Ettlingen, Germany) was adopted. Particle size distribution and shape were also measured via a particle size analyzer (Malvern MS 20, Malvern, UK) and a scanning electron microscope (SEM S-4200, Hitachi, Hitachnaka, Japan). For conductivity measurements, pellets of each sample were prepared, and then a picoammeter (Keithley 487, Cleveland, USA) with a custom-made cell (two probes) was applied.

The ER fluids of PPP particles dispersed in silicone oil (poly(dimethylsiloxane); kinematic viscosity of 30 cSt) were prepared by the mixture at 1500−1800 rpm using a custom-made pearl mill (Shinil Co., Korea). Characteristics of various ER fluids investigated in this paper are given in Table 1. Depending on the doping degree, the samples were indexed to be PPP-(0.0), PPP(2.5), PPP(5.0), and PPP(7.5) for undoped, doped with 2.5 wt % $FeCl_3$, 5.0 wt % $FeCl_3$, and 7.5 wt % $FeCl_3$ in aqueous solutions, respectively.

Rheological Measurement. Experiments were carried out using a rotational rheometer (Physica MC120, Stuttgart, Germany) with a Couette geometry (Z3-DIN and Z4-DIN), a high-voltage generator (HVG 5000, Stuttgart, Germany), and an oil bath for temperature control. The gaps of the Z3-DIN and the Z4-DIN were 1.06 and 0.59 mm, and their maximum measurable stresses were 1.141 and 6.501 kPa, respectively. The HVG 5000 could supply dc voltage up to 5 kV within ±10 μA of electric current. Temperature could be controlled from −40 to 150 °C. The suspensions were placed in the gap between the stationary outer measuring cup and the rotating bob.

An electric field was applied for 3 min to obtain an equilibrium chainlike or columnar structure before applying shear. To obtain reproducible data, ER fluids were redispersed

(18) Otsubo, Y.; Sekine, M.; Katayama, S. *J. Colloid Interface Sci.* **1992**, *150*, 324.
(19) Wu, C. W.; Conrad, H. *Int. J. Mod. Phys. B* **1999**, *13*, 1713.
(20) Choi, H. J.; Cho, M. S.; Kang, K.-K.; Ahn, W.-S. *Microporous Mesoporous Mater.* **2000**, *39*, 19.
(21) Ikazaki, F.; Kawai, A.; Uchida, K.; Kawakami, T.; Sakurai, K.; Anzai, H.; Asako, Y. *J. Phys. D: Appl. Phys.* **1998**, *31*, 336.
(22) Negita, K.; Ohsawa, Y. *J. Phys. II* **1995**, *5*, 883.
(23) Cho, M. S.; Choi, H. J.; Chin, I.-J.; Ahn, W.-S. *Microporous Mesoporous Mater.* **1999**, *32*, 233.
(24) Böse, H. *Int. J. Mod. Phys. B* **1999**, *13*, 1878.
(25) Kojima, Y.; Matsuoka, T.; Takahashi, M. *J. Appl. Polym. Sci.* **1994**, *53*, 1393.
(26) Cho, M. S.; Kim, T. W.; Choi, H. J.; Jhon, M. S. *J. Macromol. Sci., Pure Appl. Chem.* **1997**, *A34*, 901.
(27) Webber, R. M. In *Progress in Electrorheology*; Havelka, K. O., Filisko, F. E., Eds.; Plenum Press: New York, 1995; p 171.
(28) Quadrat, O.; Stejskal, J.; Kratochvíl, P.; Klason, C.; McQueen, D.; Kubát, J.; Sáha, P. *Synth. Met.* **1998**, *97*, 37.
(29) Lee, J. H.; Cho, M. S.; Choi, H. J.; Jhon, M. S. *Colloid Polym. Sci.* **1999**, *277*, 73.
(30) Choi, H. J.; Lee, Y. H.; Kim, C. A.; Jhon, M. S. *J. Mater. Sci. Lett.* **2000**, *19*, 533.
(31) Cho, M. S.; Choi, H. J.; To, K. *Macromol. Rapid Commun.* **1998**, *19*, 271.
(32) Choi, H. J.; Kim, J. W.; To, K. *Synth. Met.* **1999**, *101*, 697.
(33) Cho, M. S.; Kim, J. W.; Choi, H. J.; Webber, R. M.; Jhon, M. S. *Colloid Polym. Sci.* **2000**, *278*, 61.
(34) Block, H.; Kelly, J. P.; Qin, A.; Watson, T. *Langmuir* **1990**, *6*, 6.
(35) Choi, H. J.; Cho, M. S.; Jhon, M. S. *Int. J. Mod. Phys. B* **1999**, *13*, 1901.
(36) Trlica, J.; Sáha, P.; Quadrat, O.; Stejskal, J. *Physica A* **2000**, *283*, 337.
(37) Choi, H. J.; Kim, J. W.; Noh, M. H.; Lee, D. C.; Suh, M. S.; Shin, M. J.; Jhon, M. S. *J. Mater. Sci. Lett.* **1999**, *18*, 1505.
(38) Kim, J. W.; Kim, S. G.; Choi, H. J.; Jhon, M. S. *Macromol. Rapid Commun.* **1999**, *20*, 450.
(39) Kim, J. W.; Noh, M. H.; Choi, H. J.; Lee, D. C.; Jhon, M. S. *Polymer* **2000**, *41*, 1229.
(40) Plocharski, J.; Rózañski, M.; Wyciœlik, H. *Synth. Met.* **1999**, *102*, 1354.
(41) Chin, B. D.; Lee, Y. S.; Park. O. O. *Int. J. Mod. Phys. B* **1999**, *13*, 1852.
(42) Choi, H. J.; Sim, I. S.; Jhon, M. S. *J. Mater. Sci. Lett.* **2000**, *19*, 1629.
(43) Kovacic, P.; Oziomek, J. *J. Am. Chem. Soc.* **1963**, *85*, 454.

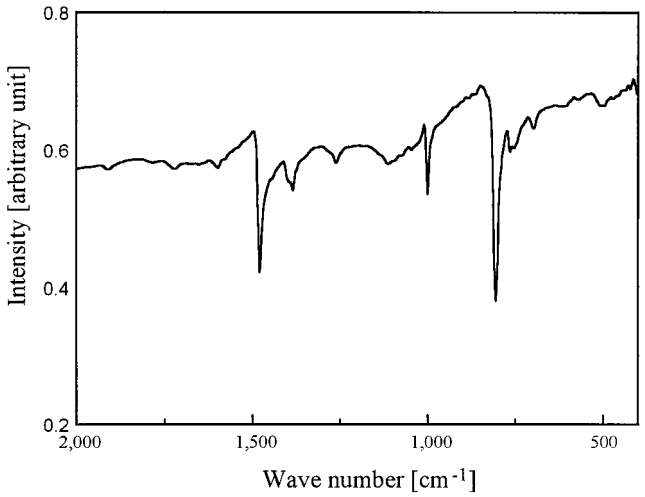

Figure 1. FT-IR spectrum of PPP.

before each experiment, and measurements were carried out at least three times. The shear rate was varied from 10^{-2} to 10^{2} s^{-1}, and yield stresses for the prepared ER fluids were mainly obtained under flow in a controlled shear rate (CSR) experiment. The stress of the transition point at which viscosity abruptly decreased was interpreted as the yield stress. Flow curves for each ER fluid were determined in the CSR mode, and static yield stresses were obtained in controlled shear stress (CSS) mode.

Results and Discussion

Characterization. The synthesized PPP was identified from the characteristic peaks of the FT-IR spectrum as shown in Figure 1 with a strong peak at 800 cm^{-1} for the C−H out-of-plane deformation of 1,4-disubstituted benzene, a peak at 1033 cm^{-1} for in-plane deformation, and peaks at 1478 and 1403 cm^{-1} for ring-stretching structure. The density of the dried PPP particles was also measured to be about 1.21 g/cm^3 using a pycnometer. Furthermore, Figure 2a shows the average particle size distribution of the PPP in the range 15−25 μm (diameter) from the particle size analyzer. The shapes of the PPP particles were also irregular for both the undoped and doped particles from the SEM photography (Figure 2b).

Obviously the conductivity varies with dopant concentration, and the doping condition may affect the rearrangement of charges in the polymer backbone. Synthesized PPP shows semiconducting behavior due to moving charge carriers that can be activated under a strong electric field strength. However, in doped PPP, interchain transport of electrons, due to the charge defect structure, could be intensified under an imposed external field. This result shows that an increase of dopant concentration leads to an increase of the synthesized particle conductivity as shown in Table 1.

Rheological Properties. Parts a and b of Figure 3 respectively show flow curves of shear stress and shear viscosity vs shear rate from the CSR experiment for 10 wt % suspensions of undoped PPP(0.0) and PPP(5.0) with different electric field strengths, in which the apparent viscosity is defined as $\eta \equiv \tau/\dot{\gamma}$. In the absence of an electric field, ER fluids behave like an ordinary dilute suspension by showing a slight departure from Newtonian fluid behavior. When an electric field is

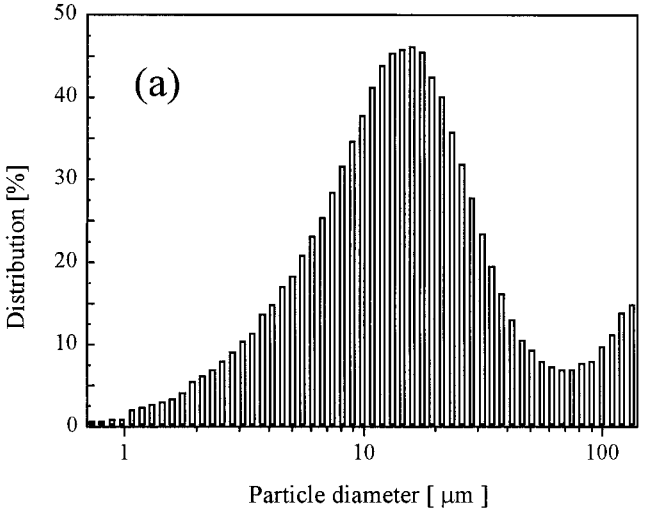

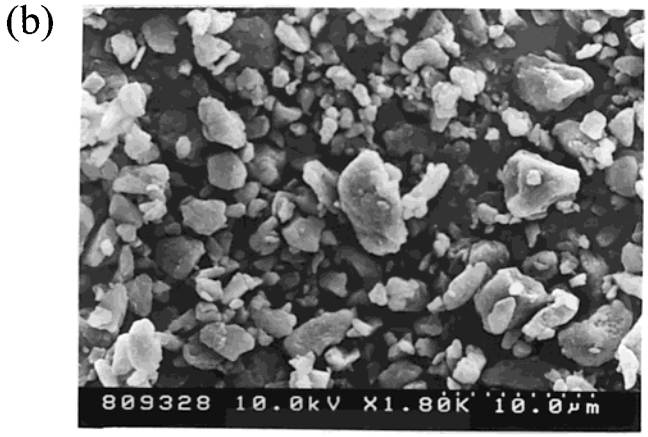

Figure 2. (a) Particle size distribution of PPP on a semilog plot and (b) SEM photography of doped PPP.

applied to the suspension, the shear stress increases with increasing electric field strength, and τ_y becomes greater than zero (like in a Bingham fluid). In general, the structure in a concentrated suspension can be sufficiently rigid to permit the material to withstand a certain level of deforming stress without flowing. The maximum stress that can be sustained without flow is the yield stress. Doped suspensions, like the undoped ones, show similar behavior, such that the shear stress increases as electric field strength increases. It could be clearly seen that the shear stress of the doped suspension is larger than that of the undoped one. Note that the rheological measurements permit investigation of only a limited frequency range and electric field strength due to deformation, power supply capacity, and conductivity breakdown. As shown in Figure 3b, the viscosity of the ER fluids exhibits power-law behavior (slope of −1). The critical shear rate ($\dot{\gamma}_c$) is defined as the discontiuity point in slope. $\dot{\gamma}_c$ of PPP is weakly dependent on electric field strength but depends on the doping degree (conductivity value) as shown in Figure 3b and Figure 4b.

Figure 4a illustrates shear stress from the CSR test for 10 wt % suspensions of PPP(0.0), PPP(2.5), PPP(5.0), and PPP(7.5) under a 3 kV/mm electric field strength. As the doping degree of PPP increases, shear stress abruptly increases between 10 and 100 s^{-1}. Each static yield stress, measured in a CSS mode, is marked as filled symbols in Figure 4a on the vertical axis. We

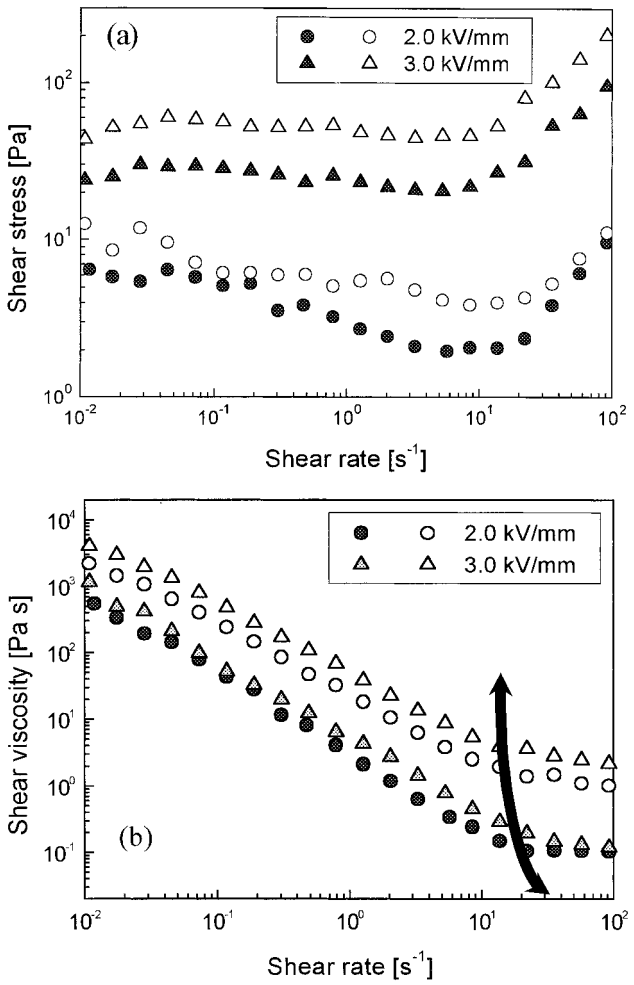

Figure 3. (a) Shear stress vs shear rate and (b) shear viscosity vs shear rate for PPP(0.0) (filled symbols) and PPP(5.0) (empty symbols) under various electric field strengths. (Circles are for 2 kV/mm and triangles for 3 kV/mm.)

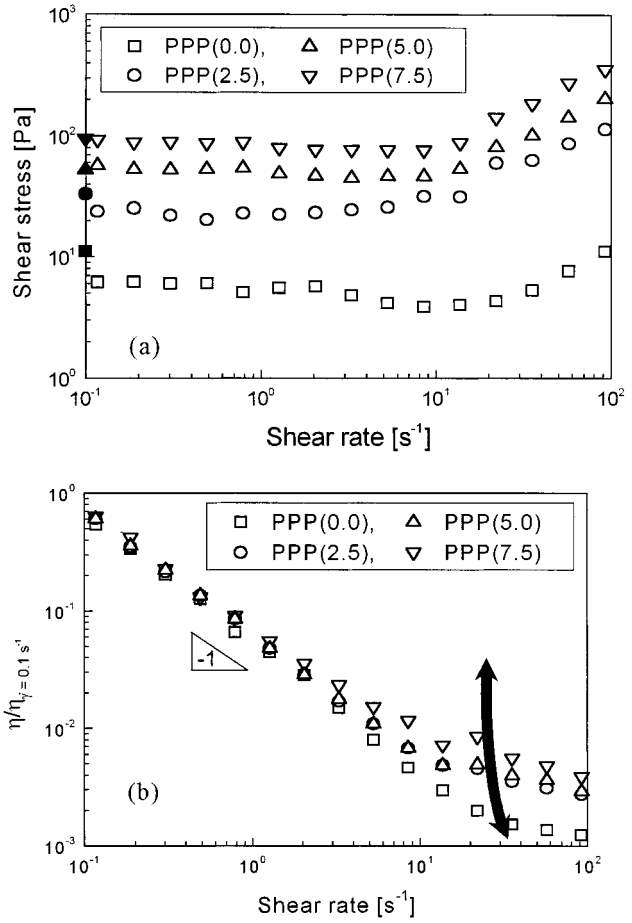

Figure 4. (a) Shear stress vs shear rate and (b) normalized shear viscosity vs shear rate for PPP(0.0), PPP(2.5), PPP(5.0), and PPP(7.5) under 3 kV/mm. The solid symbols on the stress axis are static yield stresses for each of the ER fluids measured by the CSS method.

normalized the shear viscosities to a shear rate of 0.1 s^{-1} to examine the power-law behavior and to determine $\dot{\gamma}_c$. Figure 4b shows that the PPP ER fluids behave like a power-law fluid with power-law index of -1, and $\dot{\gamma}_c$ decreases as the doping degree increases.

A correlation between the yield stress and electric field strength is represented in Figure 5a. τ_y is enhanced with the doping degree. On a log plot, the data show a linear relationship to the electric field strength (slope of 1.5).

To present the yield stress data for the broad range of electric field strength, Choi et al.[44] introduced the following simple yield stress equation:

$$\tau_y(E_0) = \alpha E_0^2 \left(\frac{\tanh\sqrt{E_0/E_c}}{\sqrt{E_0/E_c}} \right) \qquad (2)$$

where α depends on the dielectric constant of the fluid and particle volume fraction, and E_c is the critical electric field strength, which is proportional to the particle conductivity. By normalizing eq 2 with E_c and $\tau_y(E_0)$, we obtained the following generalized scaling function:[44]

$$\hat{\tau} = 1.313\hat{E}^{3/2} \tanh\sqrt{\hat{E}} \qquad (3)$$

where $\hat{E} \equiv E_0/E_c$ and $\hat{\tau} \equiv \tau_y(E_0)/\tau_y(E_c)$. The PPP data are collapsed onto a single curve using eq 3, which is shown in Figure 5b. E_c is 1.5 kV/mm for PPP(0.0), 1.2 for PPP(2.5), 1.0 for PPP(5.0), and 0.9 for PPP(7.5).

Dynamic oscillatory measurements were also performed, and these were used to study the viscoelastic properties of the solidified ER fluid under an applied electric field. The strain amplitude sweep test, which is a measurement of stress as a function of sinusoidal strains at a constant frequency, was initially attempted to find a linear viscoelastic region.

Figure 6 shows storage modulus (G') from the dynamic test for a 10 wt % suspension of PPP(7.5) with three different electric field strengths (1.0, 2.0, and 3.0 kV/mm) and a strain of 0.0125. G' remained unchanged over a broad frequency range (up to 628 Hz) and increased with electric field strength. This is the typical behavior of cross-linked rubbers,[12] which do not relax in a given frequency range. Because the relaxation time for deformation was too long, it is expected that the internal chain structures of ER fluids are not destroyed by deformation under the given conditions. Note that G' arises entirely from the nonhydrodynamic,[16] electrostatic interactions, creating tension along the chain. At a high-frequency range, G' increased slightly, showing

(44) Choi, H. J.; Cho, M. S.; Kim, J. W.; Kim, C. A.; Jhon, M. S. *Appl. Phys. Lett.*, submitted.

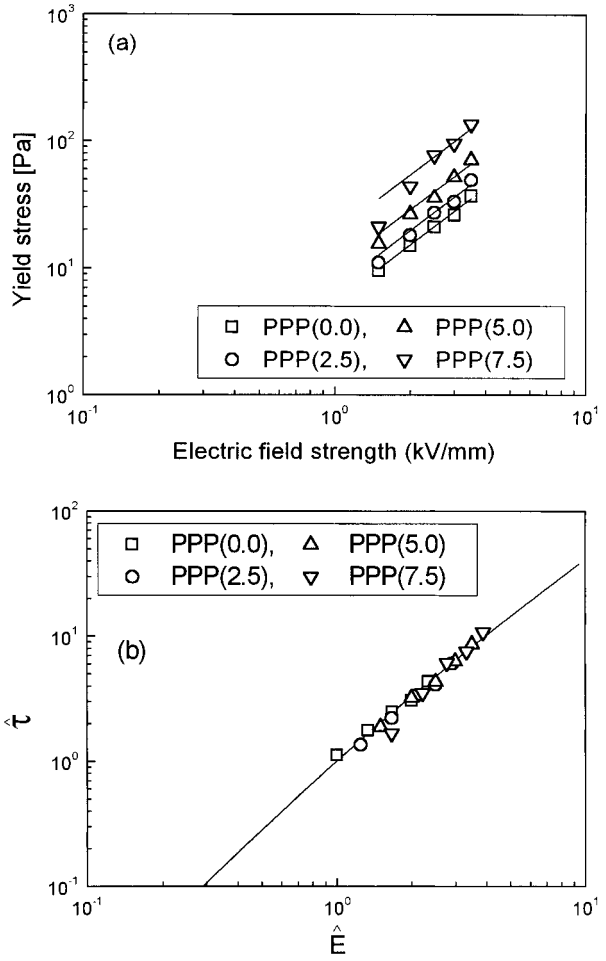

Figure 5. (a) Yield stress vs electric field strength and (b) $\hat{\tau}$ vs $\hat{E}$ for PPP(0.0), PPP(2.5), PPP(5.0), and PPP(7.5).

a transition to a nonlinear region due to the onset of chain breaking. Also, we observed the effect of electric field strength on viscoelastisity of the ER fluids.

Figure 7 shows G' with a small strain in linear viscoelastic region.[45] G' is independent of frequency but increases with doping degree (i.e., conductivity). However, the low doping degree, 2.5 and 5.0 wt % doped PPP, suspensions show an unstable, fluctuating value.

Conclusion

Rheological properties of the suspension were examined in a broad range of electric field strength and doping degrees. The suspensions of PPP in silicone oil show a striking increase in the apparent viscosity upon the application of electric field. Conductivity of PPP was increased with doping degree. The shear stress and

(45) Ahn, K. H.; Klingenberg, D. J. *J. Rheol.* **1994**, *38*, 713.

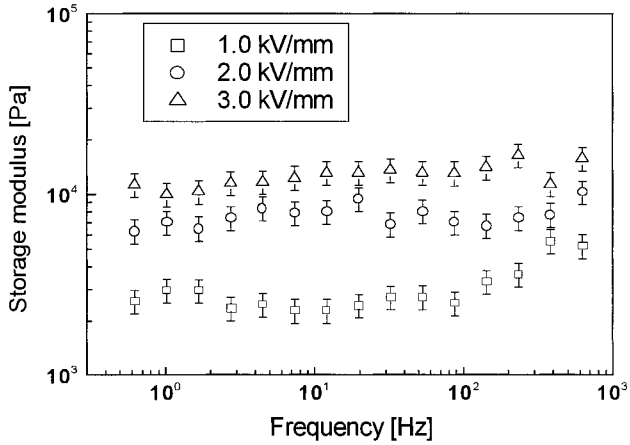

Figure 6. Storage modulus vs frequency for PPP(7.5) under various electric field strengths (strain = 0.0125).

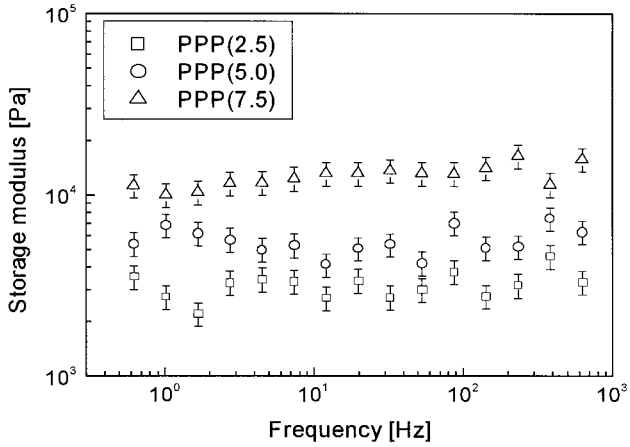

Figure 7. Storage modulus vs frequency for PPP(2.5), PPP-(5.0), and PPP(7.5) under 3 kV/mm (strain = 0.0125).

shear viscosity increased with electric field strength, weight fraction, and doping degree. The critical shear rate decreases as the doping degree increases. The yield stress of PPP suspensions increased with electric field strength and was enhanced by higher conductivity. τ_y is proportional to $E_0^{1.5}$, regardless of the doping degree. The yield stresses of PPP fit the universal scaling curve. The data reported in this paper are for $E_0 > E_c$. (All of PPP suspensions exhibit nonlinear conductivity.) From the dynamic tests, the storage modulus increased with electric field strength, weight fraction, and doping degree but remained unchanged value in the measuring frequency range.

Acknowledgment. This study was supported by grant from the KOSEF through Applied Rheology Center at Korea University, Korea.

CM000677L